

# The International Journal of Robotics Research

<http://ijr.sagepub.com>

---

## On the Kinematic Design of Spherical Three-Degree-of-Freedom Parallel Manipulators

Clément M. Gosselin and Eric Lavoie

*The International Journal of Robotics Research* 1993; 12; 394

DOI: 10.1177/027836499301200406

The online version of this article can be found at:  
<http://ijr.sagepub.com/cgi/content/abstract/12/4/394>

---

Published by:

 SAGE Publications

<http://www.sagepublications.com>

On behalf of:



Multimedia Archives

Additional services and information for *The International Journal of Robotics Research* can be found at:

**Email Alerts:** <http://ijr.sagepub.com/cgi/alerts>

**Subscriptions:** <http://ijr.sagepub.com/subscriptions>

**Reprints:** <http://www.sagepub.com/journalsReprints.nav>

**Permissions:** <http://www.sagepub.com/journalsPermissions.nav>

Clément M. Gosselin

Eric Lavoie

Département de Génie Mécanique

Université Laval

Ste-Foy, Québec, Canada, G1K 7P4

# On the Kinematic Design of Spherical Three-Degree-of-Freedom Parallel Manipulators

## Abstract

*This article studies the kinematic design of different types of spherical three-degree-of-freedom parallel manipulators. The mechanical architectures presented have been introduced elsewhere. However, designs having at least one isotropic configuration are suggested here for the first time. Isotropic configurations are defined, in turn, as those configurations in which the Jacobian matrix, mapping the angular velocity vector of the effector into the joint velocities, is proportional to an orthogonal matrix. First, a review of the direct and inverse kinematics of spherical three-degree-of-freedom parallel manipulators is outlined, and a general form for the Jacobian matrix is given. Parallel manipulators with revolute or prismatic actuators are discussed. Then, the concept of kinematic conditioning is recalled and used as a performance index for the optimization of the manipulators. It is shown that this leads to designs having at least one isotropic configuration. Finally, a few examples of such designs are presented.*

## 1. Introduction

During the past decade, many researchers have been working on parallel manipulators or parallel architecture mechanisms (Hunt 1983; Fichter 1986; Merlet 1987; Gosselin 1988). These manipulators can be used to replace conventional serial robots when better stiffness is needed and a large workspace is not necessary.

One of the designs proposed consists of a spherical parallel manipulator used to orient a rigid body in space (Asada and Cro Granito 1985; Gosselin and Angeles 1989; Craver 1989). Other kinds of similar mechanisms have also been proposed in Kurtz and Hayward (1991). Spherical manipulators can be used, for example, for the

orientation of solar panels or parabolic antennas as well as for the orientation of machine tool beds and workpieces. Such a manipulator could also be applied as an orientation wrist in an industrial robot. Moreover, an application in biomechanical engineering (i.e., to replace existing artificial hips) is currently being studied.

The purpose of this article is to present different kinds of spherical parallel manipulators and to show how their kinematic design could be optimized to obtain manipulators with isotropic configurations. To this end, the direct and inverse kinematics will be reviewed. Then, a general form for the Jacobian matrix will be given for manipulators with either revolute or prismatic actuators. Finally, it will be shown that it is possible to obtain spherical parallel manipulators having isotropic configurations by properly adjusting the geometric parameters. In these configurations, the designs then obtained lead to the best possible kinematic accuracy at the effector for a given accuracy of the actuators (Salisbury and Craig 1982).

For all the manipulators discussed, symmetric configurations will be assumed for the base and the gripper, not only to simplify the equations, but also to consider the most general applications. Indeed, because the tasks to be performed are not known a priori, it seems natural to consider a symmetric design.

## 2. Kinematic Architectures

### 2.1. Spherical Parallel Manipulators With Revolute Actuators

The manipulators studied in this section consist of three identical kinematic subchains connecting the base to a common end effector. On each chain, there is one fixed actuated revolute joint whose rotation is associated with angle  $\theta_i$ , and two free revolute joints connecting, respectively, the proximal and distal links and the distal link with the end effector. The rotation of the two free joints are represented by angles  $\phi_i$  and  $\delta_i$ , respectively.

---

Eric Lavoie is currently at Laboratoire de Robotique, Institut de Recherche d'Hydro-Québec 1800 Montée Ste-Julie, Varennes, Québec, Canada, J3X 1S1.

The International Journal of Robotics Research,  
Vol. 12, No. 4, August 1993, pp. 394–402,  
© 1993 Massachusetts Institute of Technology.

The characteristic feature of all spherical three-degree-of-freedom manipulators with revolute joints is that the axes of rotation of all the joints intersect at a common point called the *geometric center* of the manipulator. Hence, the center is the point around which every element of the robot rotates. The relative orientation of each of the axes will be used to define different types of manipulators.

### 2.1.1. Type 1: Shoulder Module

This type of manipulator is referred to in Craver (1989) as a robotic shoulder module. In this work, a complete prototype is discussed and analyzed from a design point of view. This architecture represents the most general case of spherical three-degree-of-freedom parallel manipulators. The base and the end effector can be thought of as two pyramidal modules having one vertex in common; this vertex is the geometric center of the robot. A manipulator of this type is shown in Figure 1. The axes of the revolute joints of the base and of the end effector are located on the edges of the pyramids. For purposes of symmetry, the triangle at the base of each pyramid will be an equilateral triangle. Angle  $\gamma_1$  is the angle between two edges of the base pyramid, and angle  $\gamma_2$  is the angle between two edges of the end effector pyramid (Fig. 2). Furthermore,  $\beta_i$  is the angle between one edge and a line passing through the center of the manipulator and perpendicular to the base of the pyramid. It is to be noted that only one of these two angles— $\gamma_i$  or  $\beta_i$ —is necessary to uniquely define the base or the platform of a manipulator, as they are related through:

$$\sin \beta_i = \frac{2\sqrt{3}}{3} \sin \frac{\gamma_i}{2}, \quad i = 1, 2. \quad (1)$$

Angle  $\gamma_i$ , the angle between two edges, may vary from one pyramid to the other in the same manipulator. Angles  $\alpha_1$  and  $\alpha_2$  represent the angular length associated with the intermediate links. Again, by symmetry, these angles will be the same on each of the subchains of the manipulator. As mentioned earlier, this geometry has been studied in detail in Craver (1989), which also includes equations for the inverse kinematics of the manipulator. Moreover, its direct kinematics have been solved using a polynomial approach in Gosselin et al. (1992b). In this reference, it is shown that the direct kinematic problem of this manipulator can lead to a maximum of eight different solutions.

### 2.1.2. Type 2: Manipulator With Coplanar Actuators

The kinematic design of this type of manipulator has been studied in detail in Gosselin and Angeles (1989).

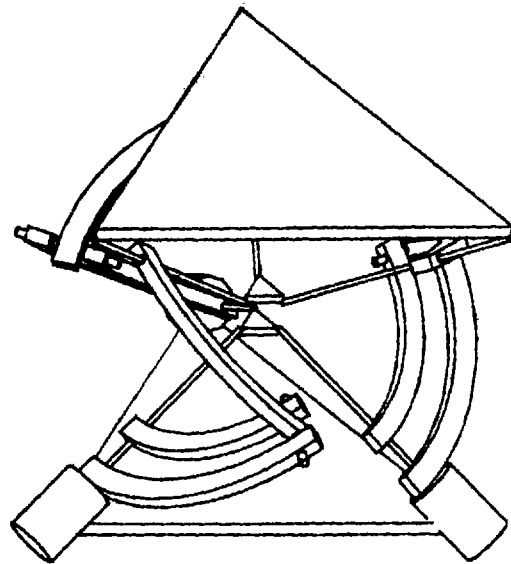


Fig. 1. Three-degree-of-freedom shoulder module.

Moreover, the direct kinematic problem has been solved using a polynomial approach in Gosselin et al. (1992a). The particular feature of this design is that the three revolute on the base and on the platform have coplanar axes. This architecture is in fact a special case of the shoulder module in which angles  $\gamma_1$  and  $\gamma_2$  are equal to  $2\pi/3$ . A manipulator of this type is represented in Figure 3.

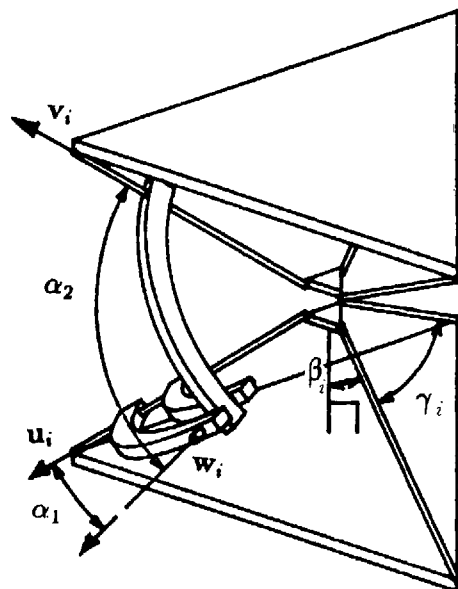


Fig. 2. Geometric parameters for the shoulder module.

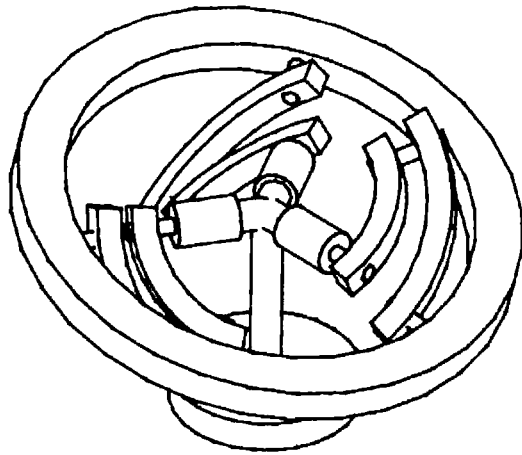


Fig. 3. Three-degree-of-freedom parallel manipulator with coplanar actuators.

### 2.1.3. Type 3: Manipulator With Collinear Actuators

The end effector of this type of spherical manipulator can take any of the configurations presented earlier. However, the base consists of three collinear actuators. This design has been briefly described in Asada and Cro Granito (1985). Once again, it is a particular case of the shoulder manipulator in which angle  $\gamma_1$  is equal to 0. Figure 4 shows a spherical manipulator with collinear actuators in which the end effector is such that angle  $\gamma_2$  equals  $2\pi/3$ . The direct kinematic problem for this type of manipulator has been studied in Gosselin et al. (1992a,b).

## 2.2. Spherical Parallel Manipulators With Prismatic Actuators

A spherical three-degree-of-freedom manipulator can also be constructed using prismatic actuators. In this case, the end effector is mounted on a fixed spherical joint—the center of rotation—and is connected to the base via three legs. Each of these legs is attached to the end effector via a spherical joint and to the base by a universal joint. Moreover, the length of the legs can be controlled using a prismatic actuator (Fig. 5). This architecture, in which the structure shown by [ABCD] is the base and [abc] is the end effector, could also be used for a three-degree-of-freedom joystick. Indeed, the prismatic actuators can be replaced by displacement transducers, which would record the length of the legs, from which the orientation of the platform can easily be computed. Such a device could be used as a master for a teleoperated spherical robot.

From a topologic point of view, the parallel manipulator with prismatic joints is exactly the same as the parallel manipulator presented in the previous section. Furthermore, the Jacobian matrix, which will be obtained later, has a similar form. One of the differences is that the

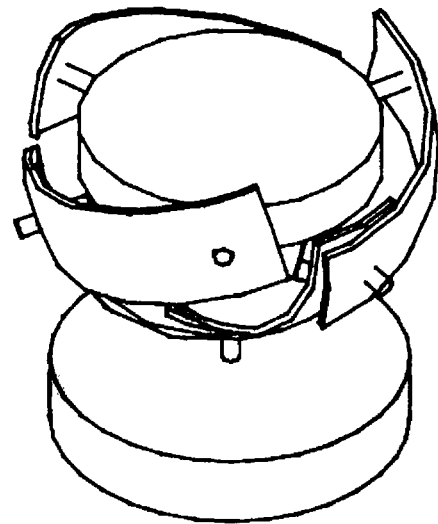


Fig. 4. Three-degree-of-freedom parallel manipulator with collinear actuators.

inverse kinematic problem leads to a unique solution in this case, whereas it leads to eight solutions in the case of the manipulator with revolute actuators. On the other hand, the direct kinematics, which have been studied in Innocenti and Parenti-Castelli (1991), leads to eight solutions, just as in the case of the manipulator with revolute actuators.

Theoretical and practical considerations lead to the conclusion that both kinematic arrangements offer potential advantages, depending on the design criteria. For example, the manipulator with prismatic actuators leads to simpler kinematic equations (a unique solution for the inverse kinematics), while the manipulator with revolute actuators leads, in general, to a larger workspace. Hence, in what follows, both cases will be investigated.

## 3. Kinematic Analysis

### 3.1. Inverse Kinematics

#### 3.1.1. Manipulator With Revolute Actuators

Because both the direct and the inverse kinematic problems have already been solved for this kind of architecture in Gosselin and Angeles (1989), Craver (1989), Innocenti and Parenti-Castelli (1991), and Gosselin et al. (1992a,b), we will now only briefly outline the results obtained for the inverse kinematics. The notation used here will be the same as the one used in Gosselin et al. (1992b). Let  $\mathbf{u}_i$ ,  $i = 1, 2, 3$  be the three unit vectors along the axes of the revolute joints of the base and let  $\mathbf{v}_i$ ,  $i = 1, 2, 3$  be the three unit vectors along the axes of the revolute joints of the end effector (see Fig. 2). The

origin of the reference coordinate frame is at the intersection of the  $\mathbf{u}_i$ s and  $\mathbf{v}_i$ s, (i.e., at the center of rotation).

In all cases studied here, the solution of the inverse kinematic problem is very simple and leads to a maximum of eight real solutions. Indeed, for manipulators with revolute actuators, we can use the following geometric constraints:

$$\mathbf{w}_i \cdot \mathbf{v}_i = \cos \alpha_2, \quad i = 1, 2, 3 \quad (2)$$

where  $\mathbf{w}_i$  is the unit vector associated to the revolute joint connecting the two intermediate members of the  $i$ th leg of the manipulator.

Moreover, when the orientation of the end effector is given (i.e., if the  $\mathbf{v}_i$ s are known), it has been shown in Craver (1989) and Gosselin et al. (1992a,b) that the solution of the above-mentioned problem will result in three uncoupled algebraic equations for the actuated joint angles—noted  $\theta_i$ ,  $i = 1, 2, 3$ —which are written as:

$$A_i T_i^2 + 2B_i T_i + C_i = 0, \quad i = 1, 2, 3 \quad (3)$$

with

$$T_i = \tan\left(\frac{\theta_i}{2}\right) \quad i = 1, 2, 3 \quad (4)$$

and

$$A_i = v_{xi}(\cos \beta_1 \cos \eta_i \sin \alpha_1 + \cos \alpha_1 \cos \eta_i \sin \beta_1) + v_{yi}(\cos \beta_1 \sin \alpha_1 \sin \eta_i - \cos \alpha_1 \sin \beta_1 \sin \eta_i) - v_{zi}(\cos \alpha_1 \cos \beta_1 + \sin \alpha_1 \sin \beta_1) - \cos \alpha_2 \quad (5)$$

$$B_i = -(v_{xi} \sin \alpha_1 \sin \eta_i + v_{yi} \cos \eta_i \sin \alpha_1) \quad (6)$$

$$C_i = v_{xi}(-\cos \beta_1 \cos \eta_i \sin \alpha_1 + \cos \alpha_1 \cos \eta_i \sin \beta_1) - v_{yi}(\cos \beta_1 \sin \alpha_1 \sin \eta_i + \cos \alpha_1 \sin \beta_1 \sin \eta_i) - v_{zi}(\cos \alpha_1 \cos \beta_1 - \sin \alpha_1 \sin \beta_1) - \cos \alpha_2 \quad (7)$$

where  $v_{xi}$ ,  $v_{yi}$ , and  $v_{zi}$  are the components of the known vector  $\mathbf{v}_i$ , and  $\alpha_1$ ,  $\alpha_2$ , and  $\beta_1$  depend on the geometry of the manipulator under study. Angles  $\eta_i$ ,  $i = 1, 2, 3$  represent the angles between the projections of the axes of the actuated revolute on the base plane of the fixed pyramid and a given reference in that plane. By symmetry, we can then write:

$$\eta_1 = 0, \quad \eta_2 = \frac{2\pi}{3}, \quad \eta_3 = \frac{4\pi}{3} \quad (8)$$

For a given orientation of the platform, we will then have two solutions for  $\theta_i$  for each leg.

### 3.1.2. Manipulator With Prismatic Actuators

As mentioned earlier, the inverse kinematic problem for the parallel spherical manipulator with prismatic actuators will be simpler and will lead to only one solution.

Let  $\rho_i$  be the length of the  $i$ th actuator and let  $\mathbf{Q}$  be the rotation matrix representing the orientation of the end effector in a coordinate frame fixed to the base. Moreover, let  $\mathbf{e}_i$  be the position vector of the point of attachment of the  $i$ th leg on the platform, expressed in a coordinate system fixed to the end effector. In addition, let  $\mathbf{s}_i$  be the position vector of the point of attachment of the  $i$ th leg to the base, given in a coordinate frame fixed to the base. We then have:

$$\rho_1 = \|\mathbf{f}_1 - \mathbf{s}_1\| \quad (9)$$

$$\rho_2 = \|\mathbf{f}_2 - \mathbf{s}_2\| \quad (10)$$

$$\rho_3 = \|\mathbf{f}_3 - \mathbf{s}_3\| \quad (11)$$

where

$$\mathbf{f}_i = \mathbf{Q}\mathbf{e}_i \quad (12)$$

As mentioned earlier and as shown in Innocenti and Parenti-Castelli (1991), it is recalled that the solution of the direct kinematic problem of the manipulator with prismatic actuators can lead to up to eight real solutions.

### 3.2. Derivation of the Jacobian Matrix for Manipulators With Revolute Actuators

The Jacobian matrix is defined as the matrix mapping the angular velocity of the end effector into the vector of actuated joint rates. Indeed, we can write

$$\dot{\boldsymbol{\theta}} = \mathbf{J}\boldsymbol{\omega}, \quad (13)$$

where  $\dot{\boldsymbol{\theta}}$  is the vector of actuated joint rates and  $\boldsymbol{\omega}$  is the vector giving the angular velocity of the end effector. From Gosselin and Angeles (1990), we have, for closed-loop kinematic chains, the following equation:

$$\mathbf{A}\boldsymbol{\omega} + \mathbf{B}\dot{\boldsymbol{\theta}} = \mathbf{0}, \quad (14)$$

which leads to

$$\mathbf{J} = -\mathbf{B}^{-1}\mathbf{A}. \quad (15)$$

Matrices  $\mathbf{A}$  and  $\mathbf{B}$  are given in Gosselin and Angeles (1990) and can be written in invariant form as

$$\mathbf{A} = \begin{bmatrix} (\mathbf{w}_1 \times \mathbf{v}_1)^T \\ (\mathbf{w}_2 \times \mathbf{v}_2)^T \\ (\mathbf{w}_3 \times \mathbf{v}_3)^T \end{bmatrix} \quad (16)$$

and

$$\mathbf{B} = \text{diag}(\mathbf{w}_1 \times \mathbf{u}_1 \cdot \mathbf{v}_1, \mathbf{w}_2 \times \mathbf{u}_2 \cdot \mathbf{v}_2, \mathbf{w}_3 \times \mathbf{u}_3 \cdot \mathbf{v}_3). \quad (17)$$

The Jacobian matrix is then easily obtained using the unit vectors associated with the revolute joints.

### 3.3. Derivation of the Jacobian Matrix for the Manipulator With Prismatic Actuators

The Jacobian matrix for this type of manipulator is now derived. Differentiating equations (9)–(11) with respect to time and then rearranging terms leads to

$$\dot{\rho} = \mathbf{J}\omega, \quad (18)$$

where

$$\dot{\rho} = \begin{bmatrix} \dot{\rho}_1 \\ \dot{\rho}_2 \\ \dot{\rho}_3 \end{bmatrix}, \quad \omega = \begin{bmatrix} \omega_1 \\ \omega_2 \\ \omega_3 \end{bmatrix} \quad (19)$$

and

$$\mathbf{J} = \begin{bmatrix} \frac{1}{\rho_1}(\mathbf{s}_1 \times \mathbf{Qe}_1)^T \\ \frac{1}{\rho_2}(\mathbf{s}_2 \times \mathbf{Qe}_2)^T \\ \frac{1}{\rho_3}(\mathbf{s}_3 \times \mathbf{Qe}_3)^T \end{bmatrix} \quad (20)$$

As expected, this matrix is very similar to the one obtained for the manipulators with revolute actuators. Hence, the kinematic optimization of this type of manipulator will be pursued similarly—i.e., by simply adjusting vectors  $\mathbf{e}_i$  and  $\mathbf{s}_i$  to obtain an orthogonal Jacobian matrix. Figure 5 shows an example of a decoupled parallel manipulator with prismatic actuators, which will be discussed in more detail in Section 6.

## 4. Kinematic Accuracy and Isotropy

The kinematic accuracy of a robot is defined as the accuracy of the Cartesian motion of the end effector of the manipulator for a given resolution of the actuators. In other words, the kinematic accuracy characterizes the

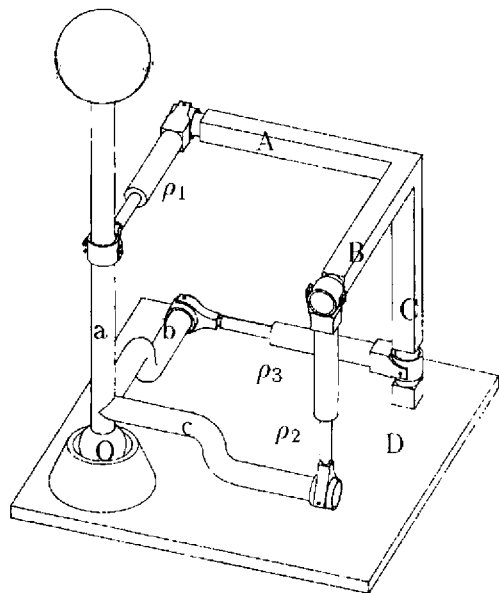


Fig. 5. Three-degree-of-freedom parallel manipulator with prismatic actuators.

natural precision of the linear system of equation (13) and (18). This concept was introduced in Salisbury and Craig (1982), where the accuracy of the linear transformation between the joint rates and the Cartesian velocities is quantified using the condition number of the Jacobian matrix, a measure used by numerical analysts (Golub and Van Loan 1983). The condition number of a matrix is defined as

$$\kappa(\mathbf{J}) = \|\mathbf{J}\| \|\mathbf{J}^{-1}\|, \quad (21)$$

and the following norm is used here:

$$\|\mathbf{J}\| = \sqrt{\text{tr}(\mathbf{J}^T \mathbf{W} \mathbf{J})}, \quad (22)$$

in which matrix  $\mathbf{W}$  is defined as

$$\mathbf{W} = \frac{1}{n} \mathbf{1}, \quad (23)$$

where  $n$  is the dimension of the square matrix  $\mathbf{J}$ , and  $\mathbf{1}$  denotes the  $n \times n$  identity matrix. Therefore, we have

$$1 \leq \kappa(\mathbf{J}) < \infty. \quad (24)$$

To simplify the numerical computations, the reciprocal of the condition number is used. Therefore, the conditioning index  $\zeta(\mathbf{J})$  is defined as

$$\zeta(\mathbf{J}) = \frac{1}{\kappa(\mathbf{J})}, \quad (25)$$

and hence

$$0 < \zeta(\mathbf{J}) < 1. \quad (26)$$

A value of  $\zeta(\mathbf{J})$  in the immediate vicinity of zero denotes a singular configuration, whereas a value in the immediate vicinity of 1 characterizes an isotropic configuration (i.e., a perfectly conditioned Jacobian matrix). Moreover, because only orthogonal matrices and their multiples are perfectly conditioned, an isotropic configuration will lead to a decoupling of the motion of the manipulator. Indeed, in such a configuration, a unit velocity of each of the three actuators will be associated with angular velocities of the end effector in three orthogonal directions, respectively, and having the same magnitude.

One of the main objectives of this work is to optimize the geometric design of parallel spherical manipulators to obtain an isotropic robot (i.e., a robot that can attain at least one isotropic configuration). This can be achieved for the type 1 manipulator (shoulder manipulator) by mere geometric reasoning. Indeed, it is clear that if each of the three vectors  $\mathbf{u}_i$ ,  $i = 1, 2, 3$  on the base are aligned with each of the three vectors  $\mathbf{v}_j$ ,  $j = 1, 2, 3$  on the platform, with  $i \neq j$ , then the motion is decoupled along orthogonal axes provided that  $\alpha_1 = \alpha_2 = \pi/2$ . Although this result is very interesting, it is, nevertheless, far from being general. Therefore, a more systematic approach to identify isotropic designs will be pursued in the next section.

## 5. Isotropy of the Spherical Parallel Manipulator

We will now attempt to obtain a set of spherical manipulators whose Jacobian matrix will be perfectly conditioned for a certain configuration. This configuration will be referred to as the *nominal configuration*. Furthermore, the nominal configuration will be assumed to be a symmetric configuration (i.e., one for which all joint variables  $\theta_i$   $i = 1, 2, 3$  are equal). We then have

$$\mathbf{B} = \begin{bmatrix} b & 0 & 0 \\ 0 & b & 0 \\ 0 & 0 & b \end{bmatrix}, \quad (27)$$

where

$$b = \frac{1}{2} \sin \alpha_1 \sin \beta \left( \sqrt{3} \cos \theta - 3 \cos \beta \sin \theta \right), \quad (28)$$

which means that if  $b$  is not equal to 0, then only matrix  $\mathbf{A}$  will affect the conditioning of the Jacobian. In addition, from the symmetry, we have:

$$\mathbf{A}\mathbf{A}^T = \begin{bmatrix} a_1 & 0 & 0 \\ 0 & a_2 & 0 \\ 0 & 0 & a_3 \end{bmatrix}, \quad (29)$$

where

$$\begin{aligned} a_1 = a_2 = & \frac{3}{2} \cos^2 \theta \sin^2 \alpha_1 (\cos^4 \beta - \cos^2 \beta \sin^2 \beta \\ & + \sin^4 \beta) \\ & - \frac{9}{2} \cos \alpha_1 \sin \alpha_1 \cos \theta (\sin^3 \beta \cos \beta \\ & - \cos^3 \beta \sin \beta) \\ & + \frac{9}{2} \cos^2 \alpha_1 \cos^2 \beta \sin^2 \beta \\ & - \frac{3\sqrt{3}}{2} \sin \theta \sin \alpha_1 (\cos \alpha_1 \cos^2 \beta \sin \beta \\ & + \cos \beta \cos \theta \sin \alpha_1 \sin^2 \beta) \\ & + \frac{3}{2} \cos^2 \beta \sin^2 \alpha_1 \sin^2 \theta \end{aligned} \quad (30)$$

and

$$\begin{aligned} a_3 = & \frac{9}{4} (\cos^2 \beta \cos^2 \theta \sin^2 \alpha_1 \sin^2 \beta + \cos^2 \alpha_1 \sin^4 \beta) \\ & - \frac{9}{2} \cos \alpha_1 \cos \beta \cos \theta \sin \alpha_1 \sin^3 \beta \\ & + \frac{3\sqrt{3}}{2} \sin \alpha_1 \sin \theta (\cos \alpha_1 \sin^3 \beta \\ & - \cos \beta \cos \theta \sin \alpha_1 \sin^2 \beta) \\ & + \frac{3}{4} \sin^2 \alpha_1 \sin^2 \beta \sin^2 \theta \end{aligned} \quad (31)$$

with, as mentioned in Section 2,

$$\beta = \sin^{-1} \left( \frac{2\sqrt{3}}{3} \sin \frac{\gamma}{2} \right). \quad (32)$$

Hence, an isotropic design will be obtained whenever the following equation is satisfied:

$$F(\alpha_1, \gamma, \theta) = a_2 - a_3 = 0 \quad \text{with } a_2, a_3 \neq 0. \quad (33)$$

The locus of the points in the  $(\alpha_1, \gamma, \theta)$  space that satisfy this equation represents the set of manipulators that are isotropic in the nominal configuration mentioned earlier. Notice that the  $(\alpha_1, \gamma, \theta)$  space has been considered instead of the more natural  $(\alpha_1, \gamma, \alpha_2)$  design space. In fact, it can be shown that both approaches are equivalent, since a unique value of  $\alpha_2$  will correspond to given values of  $\alpha_1, \gamma$ , and  $\theta$ . The former design space has been used mainly for purposes of simplicity of the equations. Figure 6 shows a number of curves obtained from equation (33) for different values of  $\gamma$ .

Because all these curves verify equation (33), they all represent loci in the design space associated with geometric parameters that lead to a perfectly conditioned Jacobian matrix. The particular case derived from geometric reasoning in the previous section appears very clearly on the graph as the curve corresponding to  $\gamma = \frac{\pi}{2}$ .

## 6. Examples

### 6.1. Manipulators With Revolute Actuators

We will now use the equation derived earlier in terms of the three design variables— $(\alpha_1, \alpha_2, \gamma)$  or, alternatively,  $(\alpha_1, \theta, \gamma)$ —to find manipulators having at least one isotropic configuration. First of all, we will fix angle  $\gamma$ , thereby imposing the geometry of the base and the platform. Then, different sets of values of  $\alpha_1$  and  $\alpha_2$  that will render the Jacobian isotropic will be considered.

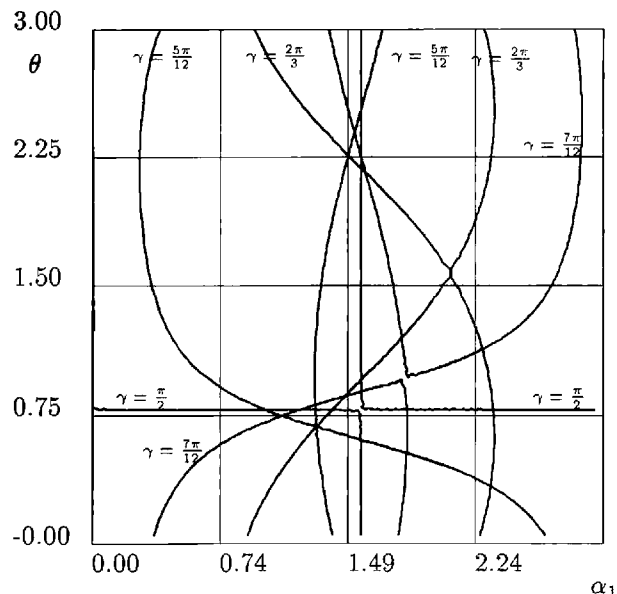


Fig. 6. Isotropic loci in the design space ( $F(\alpha_1, \gamma, \theta) = 0$ ).

6.1.1. Case 1:  $\gamma = \frac{\pi}{2}$

By imposing that  $\gamma_1 = \gamma_2 = \gamma = \pi/2$ , we obtain a shoulder module whose unit vectors  $\mathbf{u}_i$  and  $\mathbf{v}_i$  form, respectively, an orthogonal base attached to the fixed link and the platform. A graph of the conditioning of the Jacobian matrix in the nominal configuration is represented in Figure 7. From this figure, it is clear that there exist values of  $\alpha_1$  and  $\alpha_2$  for which a perfect conditioning is achieved. Moreover, for the case at hand, eq. (33) now takes on the following simplified form:

$$F(\alpha_1, \gamma, \theta) = \frac{3\sqrt{2}}{2} \cos \alpha_1 \sin \alpha_1 (\cos \theta - \sin \theta) = 0. \quad (34)$$

Hence, with the following assumption on  $\alpha_1$ —i.e.,

$$\alpha_1 = \frac{n\pi}{2} \quad n = 1, 2, 3, \dots, \quad (35)$$

the manipulator's Jacobian matrix is perfectly conditioned in the nominal configuration for any value of  $\alpha_2$ . Equation (34) is also satisfied when  $\theta$  is equal to  $\pi/4$ . However, this solution corresponds to a manipulator whose Jacobian matrix is equal to  $\mathbf{0}$ . Indeed, in this case, we have

$$a_2 = a_3 = 0, \quad (36)$$

and the condition associated with eq. (33) is not verified.

The isotropic manipulator identified using geometric reasoning in the preceding section is obtained by setting  $\alpha_2 = \pi/2$ . The corresponding Jacobian matrix is written as

$$\mathbf{J} = \begin{bmatrix} \frac{\sqrt{6}}{3} & -\frac{\sqrt{6}}{6} & -\frac{\sqrt{6}}{6} \\ 0 & \frac{\sqrt{2}}{2} & -\frac{\sqrt{2}}{2} \\ -\frac{\sqrt{3}}{3} & -\frac{\sqrt{3}}{3} & -\frac{\sqrt{3}}{3} \end{bmatrix}, \quad (37)$$

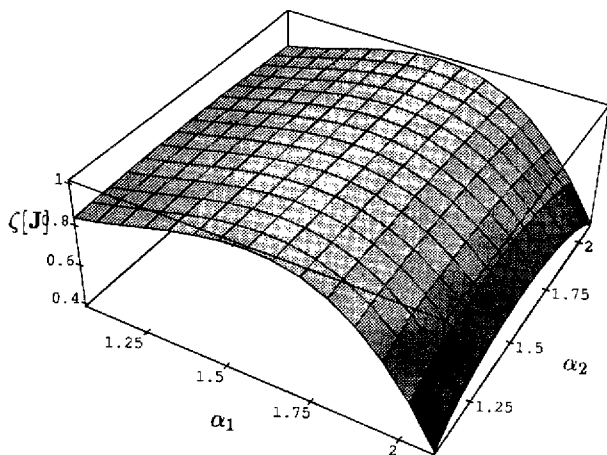


Fig. 7. Conditioning graph of the manipulator for which  $\gamma = (\pi/2)$  as a function of  $\alpha_1$  and  $\alpha_2$ .

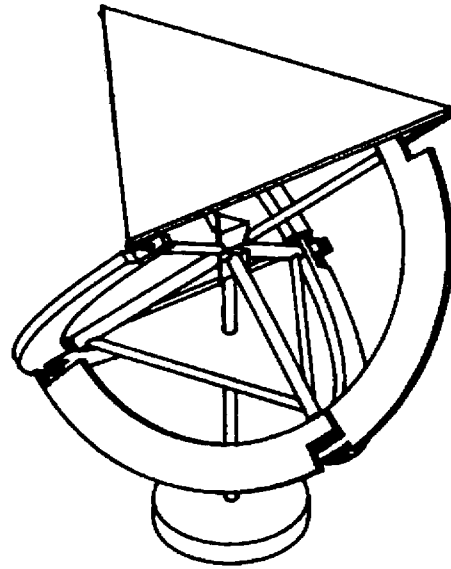


Fig. 8. Isotropic shoulder module.

which is orthogonal since

$$\mathbf{J}\mathbf{J}^T = \begin{bmatrix} 1 & 0 & 0 \\ 0 & 1 & 0 \\ 0 & 0 & 1 \end{bmatrix}. \quad (38)$$

The Jacobian matrix is then decoupled around the axes corresponding to the unit vectors  $\mathbf{v}_1, \mathbf{v}_2$  and  $\mathbf{v}_3$ . Figure 8 shows a shoulder type manipulator in an isotropic configuration with  $\alpha_1$  and  $\alpha_2$  equal to  $\pi/2$ . Another property of this manipulator is that the conditioning decreases very slowly when one moves away from the isotropic configuration. Thus, the average conditioning is very good for a finite region of the workspace centered on that configuration.

6.1.2. Case 2:  $\gamma = \frac{2\pi}{3}$

We will now consider the case for which angle  $\gamma$  is equal to  $2\pi/3$  (i.e., the spherical parallel manipulator with coplanar actuators). Figure 9 shows the conditioning of the Jacobian matrix in the nominal configuration as a function of  $\alpha_1$  and  $\alpha_2$ . It is clear from this figure and from Figure 6 that there exist points where  $\zeta(\mathbf{J}) = 1$  is satisfied. Now let

$$\alpha_1 = \frac{2\pi}{3}. \quad (39)$$

A maximum value of  $\zeta(\mathbf{J})$  is then obtained if

$$\alpha_2 = \frac{\pi}{2}. \quad (40)$$

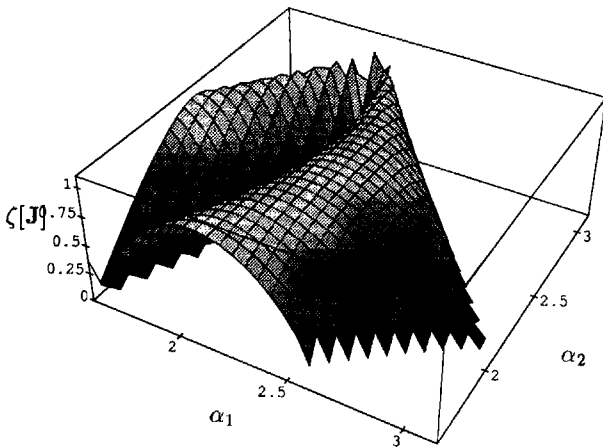


Fig. 9. Conditioning graph of the manipulator for which  $\gamma = (2\pi/3)$  as a function of  $\alpha_1$  and  $\alpha_2$ .

The corresponding manipulator is isotropic. The Jacobian matrix is written as

$$\mathbf{J} = \begin{bmatrix} 1 & -1 & 0 \\ \frac{\sqrt{3}}{3} & \frac{\sqrt{3}}{3} & -\frac{2\sqrt{3}}{3} \\ -\frac{\sqrt{6}}{3} & -\frac{\sqrt{6}}{3} & -\frac{\sqrt{6}}{3} \end{bmatrix}, \quad (41)$$

which leads to

$$\mathbf{J}\mathbf{J}^T = \begin{bmatrix} 2 & 0 & 0 \\ 0 & 2 & 0 \\ 0 & 0 & 2 \end{bmatrix}. \quad (42)$$

Figure 10 shows an isotropic spherical parallel manipulator with coplanar actuators for which  $\alpha_1 = 2\pi/3$  and  $\alpha_2 = \pi/2$ . To avoid mechanical interference between each of the legs, the links have been designed in such a way that each of the links is rotating on the surface of a different concentric sphere.

Although spherical parallel manipulators have been studied in the past, isotropic architectures such as the ones introduced here have never been obtained before. It

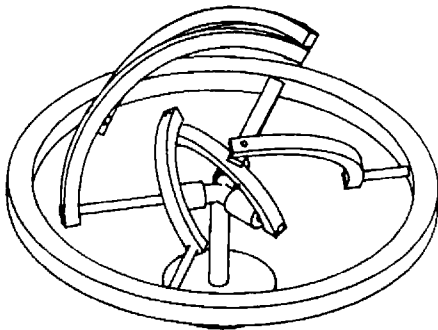


Fig. 10. Isotropic manipulator with coplanar axes.

is worth mentioning, however, that the design proposed in Craver (1989) is close to being isotropic. An isotropic spherical parallel manipulator is currently being designed at Laval University. It will be used to orient a camera with high speed and precision.

### 6.1.3. Case 3: $\gamma = \frac{7\pi}{12}$

Another example is now given. Let us impose an angle  $\gamma$  of  $7\pi/12$ . Moreover, let angle  $\alpha_1$  be equal to  $\pi/2$ . From Figure 6 and from the graphic representation of the conditioning given in Figure 11, it can be inferred that an angle of  $\alpha_2$  equal to

$$\alpha_2 = 1.84284 \simeq \frac{7\pi}{12}, \quad (43)$$

will lead to an isotropic design, because the Jacobian matrix in the nominal configuration is such that

$$\mathbf{J}\mathbf{J}^T = \begin{bmatrix} \frac{11}{10} & 0 & 0 \\ 0 & \frac{11}{10} & 0 \\ 0 & 0 & \frac{11}{10} \end{bmatrix}. \quad (44)$$

## 6.2. Manipulators With Prismatic Actuators

Because the geometry of these manipulators is very simple, an isotropic design can be identified by inspection of equations (9)–(12) and (18)–(20). Indeed, if we define the nominal configuration as the one for which

$$\mathbf{Q} = \begin{bmatrix} 1 & 0 & 0 \\ 0 & 1 & 0 \\ 0 & 0 & 1 \end{bmatrix}, \quad (45)$$

and if we impose the following geometry—i.e.,

$$\mathbf{e}_1 = \begin{bmatrix} 0 \\ 0 \\ 1 \end{bmatrix} \quad \mathbf{e}_2 = \begin{bmatrix} 1 \\ 0 \\ 0 \end{bmatrix} \quad \mathbf{e}_3 = \begin{bmatrix} 0 \\ 1 \\ 0 \end{bmatrix} \quad (46)$$

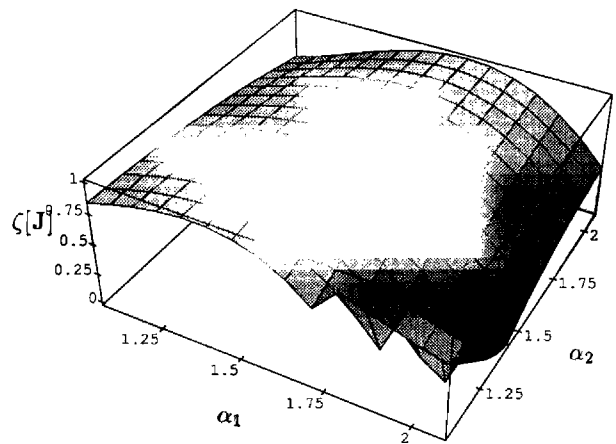


Fig. 11. Conditioning graph of the manipulator for which  $\gamma = (7\pi/12)$  as a function of  $\alpha_1$  and  $\alpha_2$ .

